Life Sciences 231 (2019) 116578

Contents lists available at ScienceDirect

Life Sciences

journal homepage: www.elsevier.com/locate/lifescie

Selenium protection against mercury neurotoxicity: Modulation of apoptosis and autophagy in the anterior pituitary

Hoda Mahmoud El Asar[a,1], Enas Ahmed Mohammed[a,b,1], Basma Emad Aboulhoda[a,*,1], Hossam Yahia Emam[a,1], Ahmad Abdel-Aliem Imam[a,1]

[a] Department of Anatomy and Embryology, Faculty of Medicine, Cairo University, Egypt
[b] Qassim University, Saudi Arabia

ARTICLE INFO

Keywords:
Selenium
Mercury
Apoptosis
Autophagy

ABSTRACT

Aims: The aim of the present study is to shed light on the modulating action of selenium on two of the most crucial cellular pathways; apoptosis and autophagy and the possible interplay between them in determining the pituitary fate in the context of mercury intoxication through demonstration of the molecular, histopathological, immunohistochemical, and ultrastructural features of selenium mercury-treated adenohypophysis.

Methods: Thirty adult *Sprague Dawley* male albino rats were assigned into control group, mercury-treated group and mercury-selenium concomitantly-treated group. The adenohypophysis was subjected to structural, molecular and protein expression assessment of autophagy and apoptotic markers and western blotted analysis of Beclin 1 as a key cross-regulator of autophagy and apoptosis.

Key findings: Selenium treatment ameliorated the mercury-induced apoptosis detected by improvement in PCR and immunohistochemical expression of the apoptotic markers Bax, Bcl-2 and Caspase-3. Selenium also improved mercury-induced autophagic dysfunction with statistically significant improvement in western blotted levels of the autophagy markers LC3I, LC3II and Beclin1. The histopathological and ultrastructural studies strongly confirmed those findings.

Significance: The crosstalk between the apoptotic Bcl-2 family of proteins and the autophagic Beclin-1LC3 pathway in the context of mercury intoxication paves the way for developing novel effective treatment strategies for several mercury-induced pituitary diseases.

1. Introduction

Mercury (Hg) is one of the most important toxins regarding human exposure. In fact, almost all living organisms are exposed to Hg. Exposure to Hg results from a multitude of several human activities including unintentional occupational exposure, ingestion in food and amalgam dental fillings. Mercury is also frequently used as an ingredient in skin products and cosmetics and as an industrial component in several pharmaceuticals and vaccine preservatives [1,2].

Despite its capability to accumulate in nearly all tissues throughout the body, mercury has special predilection to accumulate in the brain. Within the brain, mercury is preferentially stored in the pituitary gland. Consecutive reports have illustrated mercury deposition in the pituitaries of laboratory animals and humans after mercury exposure by various routes [3–6] and autopsy studies have even revealed that the pituitary retains and accumulates more inorganic mercury than the kidneys [7].

At the cellular level, recent evidence has shed light on the effect of Hg exposure on cellular structures via DNA damage [8,9] and apoptosis [10,11].

One of the cardinal mechanisms determining the cell fate of apoptosis and autophagy is the collaboration between the Bcl-2 family of proteins and the Beclin-1 pathways.

The Bcl-2 family is the best characterized protein family acting as essential regulators and effectors in programmed cell death through determining commitment of cells to apoptosis. This family consists of anti-apoptotic and pro-apoptotic members. The anti-apoptotic members of this family (e.g. Bcl-2) prevent apoptosis either by sequestering proforms of death-driving cysteine proteases called caspases (the most fundamental executioner of which is caspase 3) or by preventing the release of mitochondrial apoptogenic factors such as cytochrome *c* into the cytoplasm [12].

* Corresponding author.
E-mail address: basma.emad@kasralainy.edu.eg (B.E. Aboulhoda).
[1] All authors contributed equally to the work.

https://doi.org/10.1016/j.lfs.2019.116578
Received 18 May 2019; Received in revised form 10 June 2019; Accepted 14 June 2019
Available online 15 June 2019

The pro-apoptotic death effectors in the Bcl-2 family on the other hand are the Bax proteins which convey various cytotoxic signals via perforating the mitochondrial outer membrane and triggering a proteolytic cascade that demolishes the cell [13].

The life-or-death decision for a cell is mainly determined via collaboration between these two factions of the BCL-2 family: the pro-survival faction, BCL-2 and the pro-apoptotic Bax subfamily. Interestingly, preferential interactions between these two fractions involve inhibition of Bax activation by BCL-2 [14].

Autophagy, the naturally-regulated intracellular degradation system, is mediated by several proteins like Beclin 1, microtubule-associated protein light chain 1(LC1) and microtubule-associated protein light chain 3(LC3) [15,16]. Beclin1 (Atg6) is a well-known fundamental regulator of autophagy. The synthesis and processing of LC3 is increased during autophagy, making it a key readout of autophagy levels in cells.

Bcl-2 does not only function as an antiapoptotic protein, but also as an anti-autophagy protein that inhibits the evolutionarily conserved autophagy protein, Beclin 1 [17]. This function of Bcl-2 in inhibiting Beclin 1-dependent autophagy assists in keeping autophagy at levels compatible with cell survival, rather than cell death [18].

The mechanistic insights into the interplay between the Bcl-2 family and the Beclin-1 autophagic network illuminate the way for understanding the physiological control of apoptosis and autophagy and manipulating the pathological consequences of their imbalance.

Understanding the molecular domains of interactions between mercury and selenium has become an emerging concern, yet, to the best of the authors' knowledge, no previous study has demonstrated the dual reciprocal interaction of mercury and selenium, on both autophagy and apoptosis in the adenohypophysis.

2. Material and methods

2.1. Experimental animals

Thirty adult *Sprague Dawley* male albino rats of strain (8–10 weeks old), weighing 170–200 g were purchased from the animal care unit of Kasr El-Ainy, faculty of medicine, Cairo University. All experimental procedures were carried out according to the National Institutes of Health guide for the care and use of Laboratory animals published by the U.S. National Institute of Health. Animals were acclimatized to standard laboratory conditions and had free access to food and water ad libitum. The experiment was approved by the ethical committee of laboratory animals at Kasr El-Ainy, Faculty of medicine, Cairo University.

2.2. Experimental design

Animals were randomly assigned into the following three groups (10 rats/group).

1. Control group.
2. Mercury-treated group: received methyl mercury (the most important organic mercury compound, in terms of human exposure) at a dose of 4 mg/kg [19] via oral gavage (the LD50 of methylmercury in rats ranges from 23.9 to 39.6 mg Hg/kg [20]. Mercury salt was dissolved in double distilled water.
3. Mercury and selenium concomitantly-treated group. Received 4 mg/kg methyl mercury and sodium biselenite (0.15 mg/100 g body weight) [21–23] administered concomitantly orally daily by gastric gavage.

All drugs were purchased from Sigma (St. Louis, MO, USA) and were administered for 4 weeks; the estimated duration for intracellular accumulation of mercury in the anterior pituitary of rats following oral administration [3]. At the end of the experimental period, the rats were sacrificed, by overdose of anesthesia via intraperitoneal injection of 40 mg/kg body weight pentobarbital. The adenohypophysis was rapidly dissected and subjected to histopathological, immunohistochemical and ultrastructural examination. Real-time polymerase chain reaction was carried out to evaluate the expression of the apoptosis-related genes Bax, Bcl-2, cytochrome C and Caspase-3, Western blotted assessment of the autophagy-related markers beclin-1, LC3I and LC3II and estimation of the enzyme activity of catalase (CAT) and glutathione peroxidase (GSH-Px) have also been performed.

2.3. Histopathological examination

The adenohypophysis was kept in 10% formalin solution and subjected to Hematoxylin and Eosin (H&E) and masson's trichrome staining after routine paraffin block and histological preparation [24].

2.4. Immunohistochemical protocol

The procedure involved the following steps [25]; 4 μm thick paraffin sections were de-waxed, dehydrated. Six sections have been obtained from each animal in the different groups. After heat-mediated antigen retrieval, endogenous peroxidase activity was inhibited by peroxidase-blocking solution (3% H_2O_2). Nonspecific binding of antibodies was blocked by incubation with protein block for 1 h (normal horse serum, 10% v/v in phosphate-buffered saline, Novocastra). Sections were then overnight incubated with rabbit polyclonal anti-Bax (ab53154, 1:50), anti-Bcl2 (ab59348, 1:100) and anti-caspase 3 (ab44976, 1:1000) primary antibodies (IHC-P, species specificity including rats) (Abcam, USA). After washing in Tris-buffered saline, sections were then incubated with the secondary antibody ImmPRESS™ HRP Anti-Rabbit IgG (Peroxidase) Polymer Detection Kit derived from horse serum (MP-7401, Vector, CA, USA). Each step was followed by adequate washing with phosphate buffered saline (PBS, 0.1 mol/L, pH 7.2–7.4). DAB was applied as a chromogen, and the sections were visualized with 3, 3-diaminobenzidine (Sigma, Aldrich.) under a microscope for color development. Negative controls were done through omission of the primary antibody in the automated staining protocol. Human colon carcinoma tissue was used as a positive control.

2.5. Quantitative histomorphometric analysis

The number of apoptotic cells, the area percentage of collagen as well as the area percentage of immunohistochemically-positive cells were estimated via the image analyzer “Lecia Qwin 500C” (Leica Imaging System Ltd., Cambridge, England) affixed to a computer with a color monitor attached to a Panasonic GP 210 video color camera. All measurements were estimated under magnification 400 inside standard measuring frame (85,550 μm2) in ten non-overlapping randomly-selected fields from ten sections of each animal by two independent observers blinded to the groups.

2.6. Electron microscopic examination

Specimens were immersed in 2.5% glutaraldehyde (pH 7.4). Semithin sections were prepared at 0.5 μm thickness and stained with 1% toluidine blue in 1% borax. Ultrathin sections were double stained with 4% uranyl acetate and 0.1% lead citrate, examined and photographed by JEOL JEM 1010 transmission electron microscope (Japan).

2.7. Real-time polymerase chain reaction (real-time PCR)

Real-time PCR (Qiagen, USA; Fermentas, USA) was used to evaluate the expression of the apoptosis-related genes (Bax, Bcl-2, cytochrome C and Caspase-3) in the adenohypophyseal tissue homogenates using a specialized thermocycler with fluorescence detection units. Total RNA extraction was isolated from the adenohypophysis tissue homogenates using RNeasy Purification Reagent (Qiagen, Valencia, CA, USA)

Table 1
Sequences of primers used in real-time PCR.

Gene		Primer sequences
Bax	Forwards	TGCTGAGTGCAATTGAGATGTTT
	Reverse	GTCTGGCAAAGTAGAAGAGGGCAA
Bcl-2	Forwards	GACGCCAAGAGGGAAACACCAGAA
	Reverse	TGAGTCCTGCATTCTATTAGTGAGGG
Cytochrome-c	Forwards	TCTGGATCCAATGGGTGATGTTGAG
	Reverse	TTTGAATTCCTCATTAGTAGCTCTTTGAG
Caspase 3	Forwards	AATTCATCAGGCCTGCCGAGG
	Reverse	GCTTGTAGGCCATGTCATCCTCA
β actin	Forwards	GGTCGGTGTGAACGGATTTGG
	Reverse	ATGTAGGCCATGAGGTCCACC

according to manufacturer's instructions. This was followed by cDNA synthesis and RT-PCR amplification using 10 mL amplification mixtures containing Power SYBR Green PCR Master Mix (Applied Biosystems, Foster City, CA, USA). Estimations were done in triplicates. Relative expression of the studied genes was calculated using the comparative threshold cycle method and values were normalized to the beta-actin gene. The relative quantification was calculated by the expression $2^{-\Delta\Delta Ct}$ and reported as fold change of the background level detected in control groups [18]. The real time-PCR primer sequences are illustrated in Table 1.

2.8. Western blot analysis for detection of the autophagy-related markers beclin-1, LC3I and LC3II

Adenohypophyseal tissue was suspended in homogenization buffer (25 mM Tris-HCl, pH¼7.0, 10% Triton-X100) containing protease inhibitors and phosphatase inhibitors (protease and phosphatase inhibitor cocktail, Calbiochem), and homogenized using a tissue homogenizer (Yellow line DI 18 basic, IKA, Germany). The supernatant was collected and used to prepare protein for Western blot analysis. Expression of beclin-1, LC3I and LC3II was analyzed by Western blot after total tissue protein determination [19]. Blotting membranes were incubated with 3% bovine serum albumin in tris-buffered saline with tween (TBST), 150 mmol/L NaCl and probed with corresponding primary antibodies of anti- beclin-1, anti-LC3I and anti-LC3II (CST, Beverly, MA, USA) at 4 °C overnight at a dilution 1:500 or 1:1000 followed by incubation with horseradish peroxidase- coupled secondary anti IgG monoclonal antibody (Santa Cruz biotechnology, USA). Immunoreactive signals of blots were detected with the enhanced chemiluminescence system (ECL plus, Amersham Pharmacia Biotechnology, Milan, Italy). Bands obtained

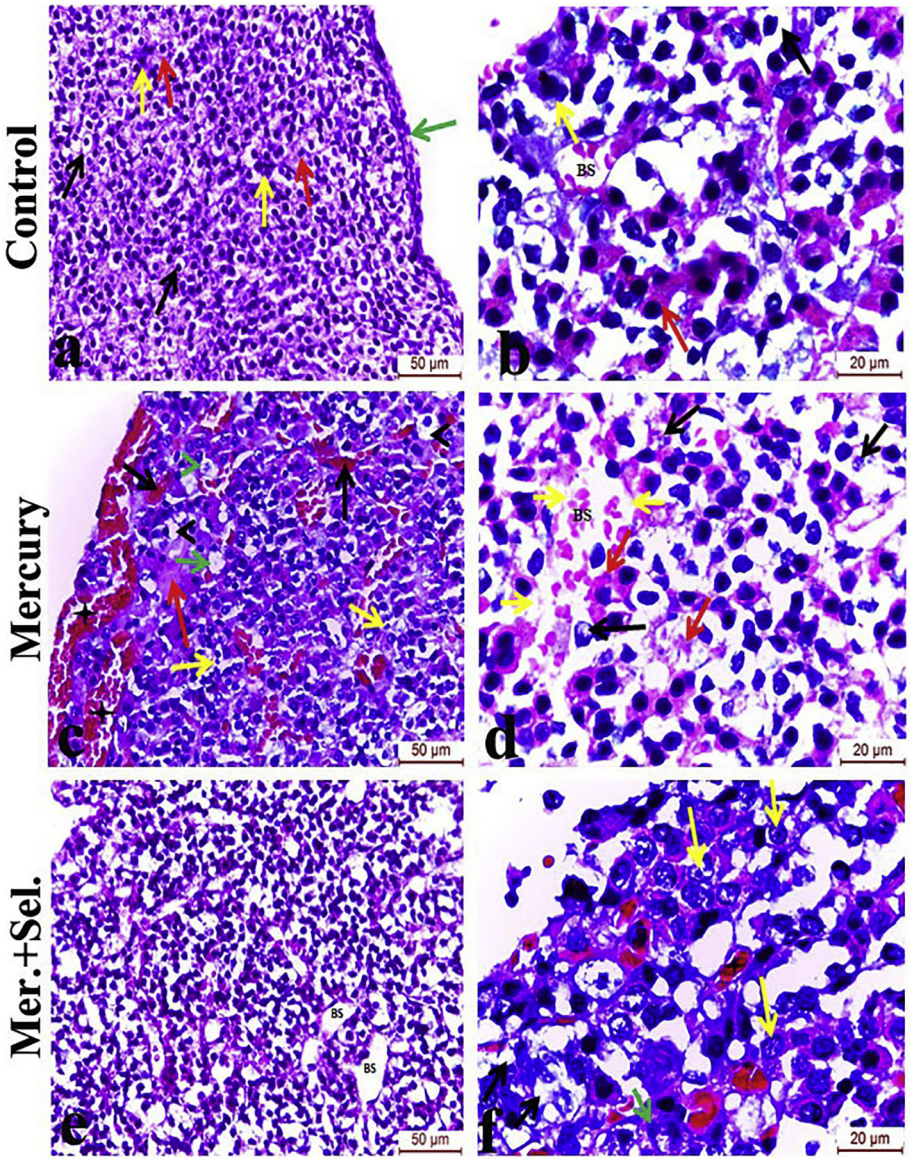

Fig. 1. H&E-stained sections of adenohypophysis of (a, b) control group showing a well-defined capsule (green arrow) and normal histological appearance of the pituitary acidophils (red arrows), basophils (yellow arrows), chromphobes (black arrows) and blood sinusoids (BS). The cells show well-defined cell boundaries. This section shows. (c) Mercury-treated group showing dilated congested blood sinusoids (black asterisks), areas of hemorrhage (black arrows) and exudation (red arrow). Some nuclei appear pyknotic (yellow arrows), others show karyolysis (green arrow). Cytoplasmic vacuolation can also be seen (black arrow heads), (d) higher magnification of the mercury-treated group showing karyorrhexis (black arrows), karyolysis (red arrows) and disruption of the wall of the blood sinusoid (BS). (e) Mercury-selenium group showing restoration of the normal architecture of the cells and blood sinusoids (BS). (f) Higher magnification of the mercury-selenium group showing healthy vesicular nuclei with prominent nucleoli (yellow arrows). (For interpretation of the references to color in this figure legend, the reader is referred to the web version of this article.)

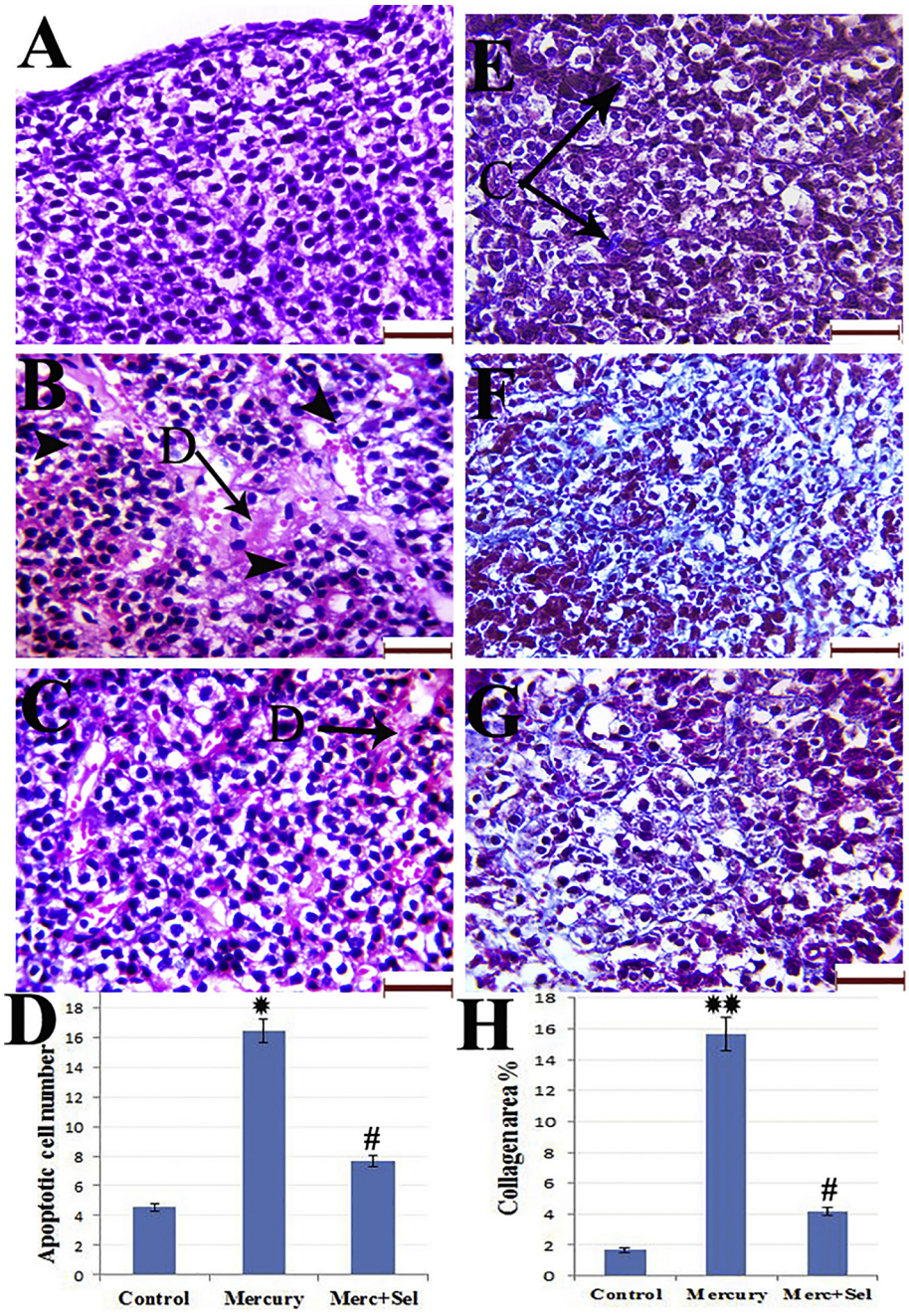

Fig. 2. A–C: H&E-stained sections of adenohypophysis of (A) control group, (B) mercury-treated group showing massive areas of degeneration (D) as well as apoptotic cells (arrow heads), (C) mercury-selenium group showing preservation of the nuclear pattern and gland architecture except for limited areas of degeneration (scale bar 50 μm) (D) bar chart representing number of apoptotic cells in the different groups.
(*: Statistically significant compared to control group, #: statistically significant compared to mercury-treated group).
E–G: Masson's trichrome-stained sections of adenohypophysis of (A) control group showing minimal collagen septa (C) (B) mercury-treated group showing extensive deposition of collagen bundles, (C) mercury-selenium group showing moderate amount of collagen fibers intervening between groups of cells (scale bar 50 μm) (D) bar chart representing area percentage of collagen.(**: highly statistically significant compared to control group, #: statistically significant compared to mercury-treated group).

from Western blot analysis were normalized against b-actin as an internal control for equal protein loading. Western blots were repeated three times for each protein.

2.9. Antioxidant enzyme activity

The activity of catalase (CAT) and glutathione peroxidase (GSH-Px) was evaluated in the pituitary homogenates using a colorimetric total mercapto (-SH) measurement assay kit (Biodiagnostic, Cairo, Egypt) as previously described [26]. The CAT activity was based upon catalyzed disappearance of 30 mM H2O2 at 240 nm while the GSH-Px activity was measured at 340 nm using GR and NADPH in a coupled reaction. One unit of GSH-Px was defined as the amount of enzyme that oxidizes 1 μmol of NADPH/min. Data were expressed as U/mg protein.

2.10. Statistical analysis

Data were analyzed using statistical package SPSS version 24. Comparisons between groups were done using ANOVA with multiple comparisons Bonferroni post hoc testing. Results were expressed as mean ± SD. P values < 0.05 and < 0.01 were considered statistically and highly-statistically significant, respectively.

3. Results

3.1. Evaluating the action of selenium on mercury-induced histopathological changes

The adenohypophysis of the mercury-treated group displayed several haemodynamic disorders including hemorrhage, exudation, dilatation, congestion and disruption of the blood sinusoids. The nuclei

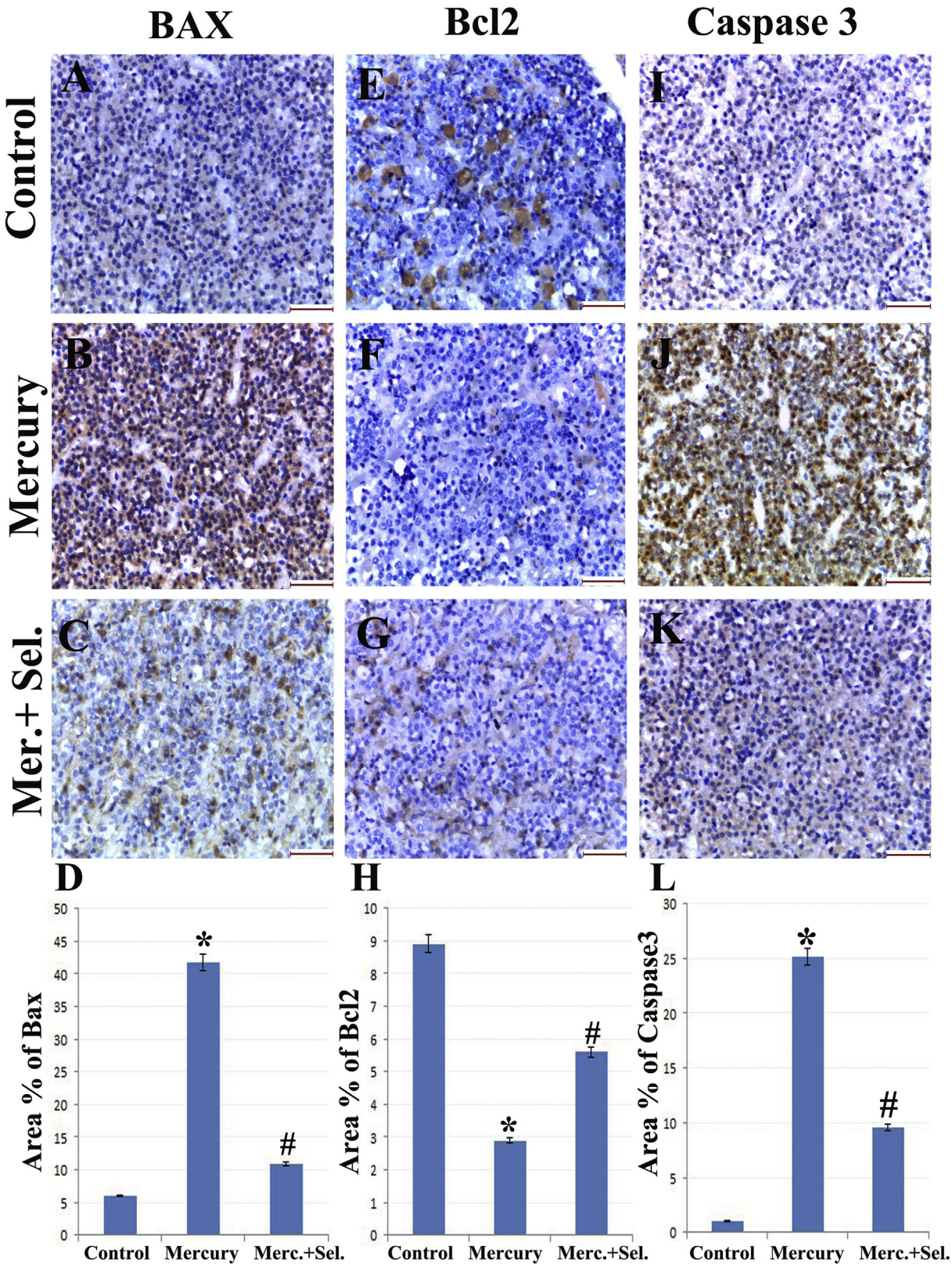

Fig. 3. Immunohistochemical expression of A–D) Bax immunohistochemistry E–H) Bcl_2 immunohistochemistry, I–L) caspase3 immunohistochemistry (scale bar 50 μm) (*: Statistically significant relative to control group, #: statistically significant compared to mercury-treated group).

showed pyknosis, karyorrhexis and karyolysi. Selenium treatment ameliorated the histopathological changes in the adenohypophysis displaying healthy gland architecture comparable to the control group (Fig. 1).

3.2. Histomorphometric results

Examination of H&E-stained sections of the mercury-treated pituitary glands revealed extensive areas of cellular degeneration together

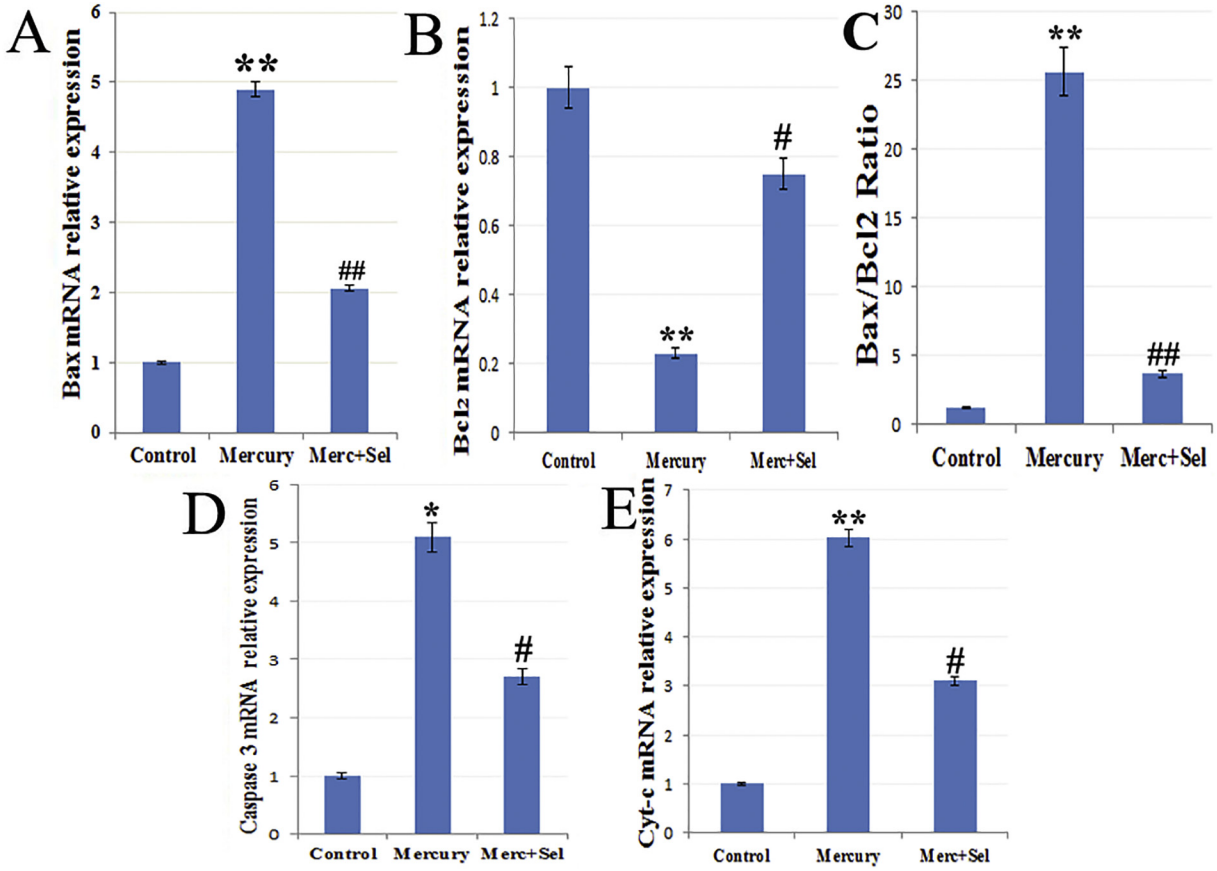

Fig. 4. PCR analysis showing the action of selenium on mRNA fold change of the apoptosis-related genes (A) Bax, (B) Bcl_2, (C) Bax/Bcl_2 ratio, (D) Caspase 3, (E) Cytochrome C.
*: Statistically significant, **: highly statistically significant compared to control group.
#: Statistically significant, ##: highly statistically significant compared to mercury-treated group.

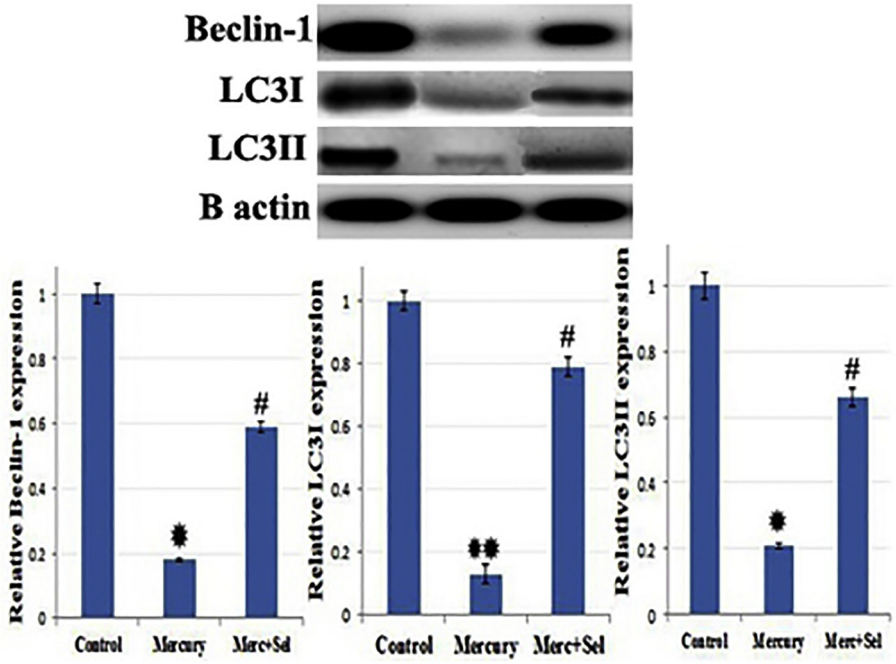

Fig. 5. Western blotting of the levels of Beclin-2, LC3I and LC3II.
(*: Statistically significant, **: highly statistically significant compared to control group, #: Statistically significant compared to mercury-treated group).

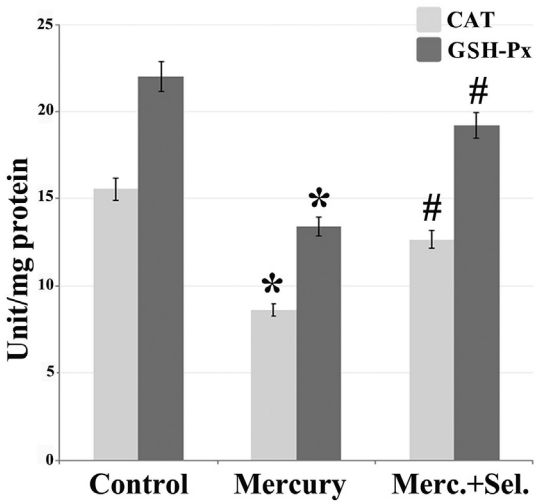

Fig. 6. The activity of the antioxidant enzymes catalase (CAT) and glutathione peroxidase (GSH-Px) (*: Statistically significant compared to control group, #: Statistically significant compared to mercury-treated group).

with statistically-significant increase in apoptotic cell count. MT-stained sections revealed marked deposition of collagen bundles upon mercury treatment. Selenium supplementation ameliorated those deleterious effects (Fig. 2).

3.3. Immunohistochemical results

Evaluation of the immunohistochemical expression of Bax, Bcl-2 and caspase-3 revealed that area percent of the apoptotic markers Bax and caspase-3 was significantly higher in the mercury-treated groups than their untreated counterparts, while the reverse was observed with the anti-apoptotic marker Bcl2. Comparing the mercury-selenium concomitantly-treated group with the mercury-treated group demonstrated significant reversal of apoptosis (Fig. 3).

3.4. Evaluating the action of selenium on apoptotic gene expression

Compared to control group, the adenohypophysis apoptotic genes expressions (Bax and caspase-3) displayed statistically-significant increase in the mercury-treated group. The mercury-selenium concomitantly-treated group showed significant reductions of those parameters when compared to the mercury-treated group. The reverse was encountered with the anti-apoptotic gene Bcl-2 (Fig. 4).

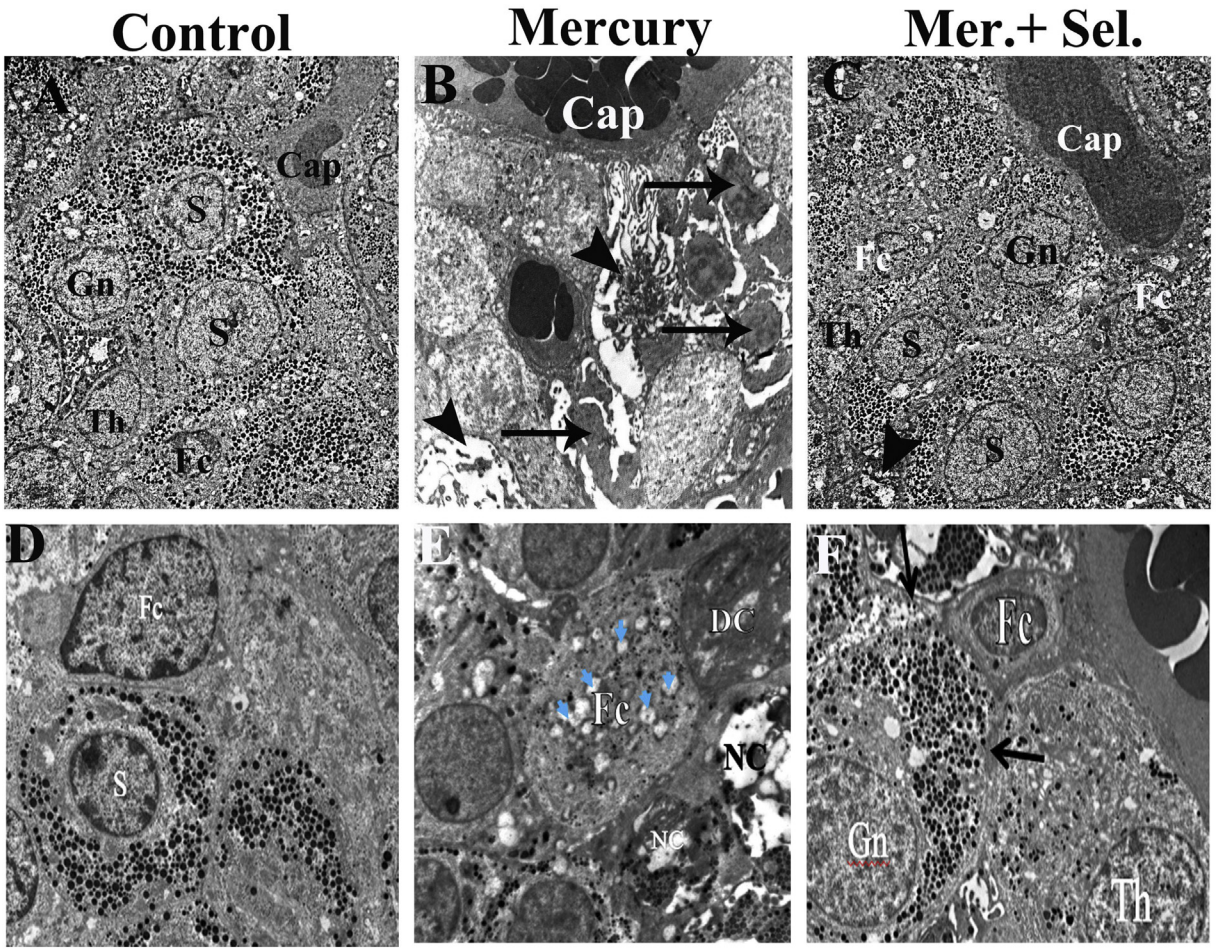

Fig. 7. Electron microscopic picture of adenohypophysis of (A) control group, (B) mercury-treated group showing autophagic vacuoles filled with cytoplasmic cargo and cellular debris (arrow heads) and apoptotic bodies (black arrows), Note: dilated congested blood capillary (cap), (C) mercury-selenium group showing reconstitution of the glandular cellular architecture with very limited areas of degeneration (arrow head) and minimal vacuolations. (D) Folliculostellate cell of the control group (E) the mercury-treated group showing a necrotic swollen folliculostellate cell (Fc) devoid of most of the cytoplasmic organelles and surrounded by degenerated (DC) and necrotic cells (NC). The cell contains large number of cytoplasmic vacuoles (blue arrows). (F) Mercury-selenium group showing healthy nucleus and intact processes (arrows) intervening between the pituicytes(A-C x 3000, D-F x 5000) (Gn: Gonadotropes, S: Somatotropes, Th: Thyrotropes, Cap: Capillaries, Fc: Folliculostellate cells). (For interpretation of the references to color in this figure legend, the reader is referred to the web version of this article.)

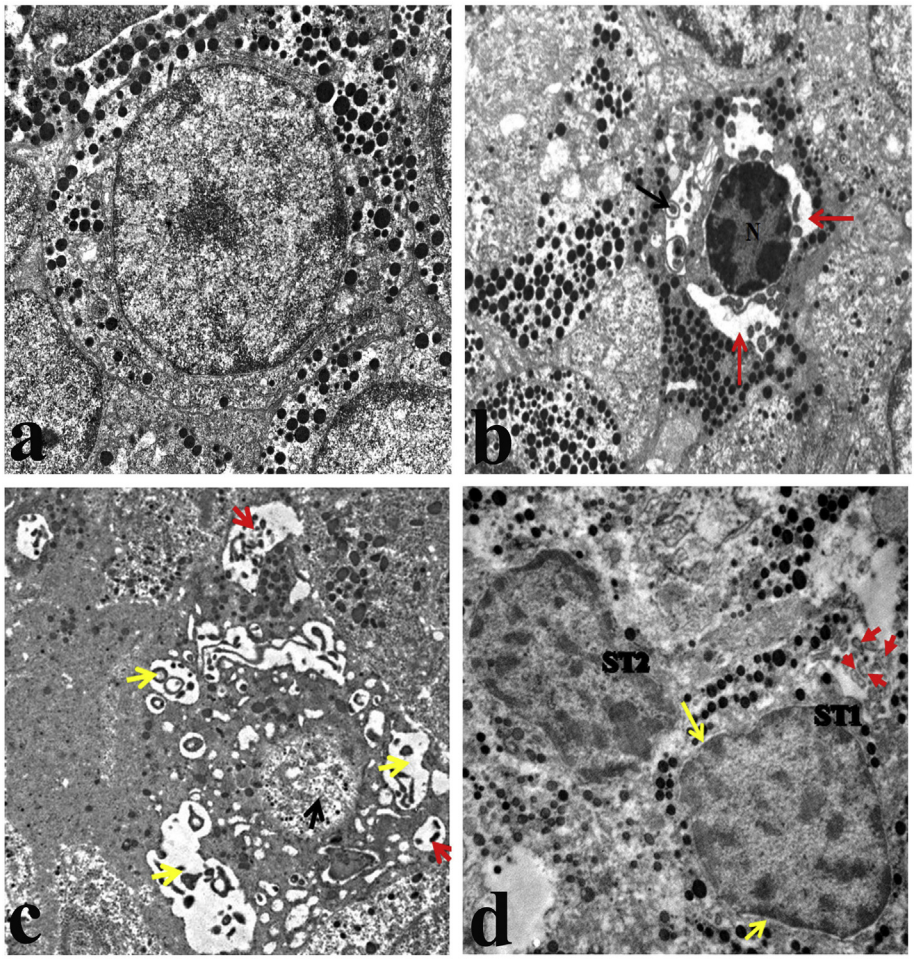

Fig. 8. Electron microscopic picture of somatotrope of (a) control group showing a somatotroph, with rounded nucleus, central nucleolus and numerous variable-sized electron-dense granules (b) mercury-treated group showing a somatotrope with an apoptotic nucleus (N), Myelin figures (black arrow) and cytoplasmic vacuolations (red arrows) with marked reduction in the number of secretory granules (c) mercury-treated group showing a degenerated somatotroph (black arrow), multivesicular bodies (red arrows) and many autophagic vacuoles (yellow arrows), (d) mercury-selenium treated group showing apparently normal somatropes (ST1, ST2) with only slightly irregular nuclear outline and widening of nuclear membrane (yellow arrows). Fragmented cytoplasmic clumps surrounded by intact membranes (red arrows) can be seen (x 6000). (For interpretation of the references to color in this figure legend, the reader is referred to the web version of this article.)

3.5. Evaluating the action of selenium on autophagy markers

The pituitary levels of beclin-1, LC3I and LC3II were significantly decreased in mercury-treated group as compared to the corresponding values of control group denoting defective autophagy. Upon selenium treatment, those values were significantly enhanced (Fig. 5).

3.6. Evaluating the action of selenium on antioxidant enzyme activity

Selenium significantly enhanced the activity of catalase (CAT) and glutathione peroxidase (GSH-Px) compared to the corresponding values of the mercury-treated group (Fig. 6).

3.7. Ultrastructural results

The mercury-treated adenohypophysis showed autophagic vacuoles filled with cytoplasmic cargo and cellular debris in addition to multiple apoptotic bodies. The folliculostellate cells were seen devoid of most of the cytoplasmic organelles and their cytoplasm contained large number of cytoplasmic vacuoles (Fig. 7). The mercury-selenium group showed preservation of the glandular cellular architecture with very minimal vacuolations (Fig. 7).

Examination of the different cellular populations revealed that mercury caused marked reduction in the number of the secretory granules of the somatropes where the cells appeared degenerated, with multivesicular bodies (red arrows) and many autophagic vacuoles. The selenium-treated soatotropes appeared healthy except for slight irregularity of the nuclear outline and widening of nuclear membrane (Fig. 8).

The gonadotropes of the mercury-treated group appeared shrunken with apoptotic nuclei, degenerated secretory granules and dilated endoplasmic reticulum cisterns. Selenium treatment refined those pathological changes (Fig. 9).

The thyrotropes of the mercury-treated group showed apoptotic nuclei with blebby nuclear membrane and cytoplasm flooded with cytoplasmic vacuoles and many lysosomes. Those changes were ameliorated with selenium treatment (Fig. 10).

4. Discussion

Despite being a research area of extreme interest, the interplay between mercury and selenium on the cellular selection between autophagy and apoptosis is still an unresolved issue [27], thus the current study has been designed to elucidate the potential modulating action of selenium on those two crucial pathways in the context of mercury toxicity in the adenohypophysis.

Enormous progress has occurred in understanding the domains of interactions between mercury and selenium including the pro-demethylating action of selenium on mercury [28], the formation of Hg-Se complex via the chelating effect of selenium on mercury [29], the redistribution of inorganic mercury inside organisms under the influence of Se [30], the inhibitory action of Se on free Hg [31], and the role of selenozymes in inhibiting mercury intoxication [32–34], yet, to the best of our knowledge, our study is the first to report the dual reciprocal interaction of mercury and selenium, on both autophagy and apoptosis in the adenohypophysis.

The current study recorded pronounced anti-apoptotic action of selenium which was illustrated by significant decrement in the

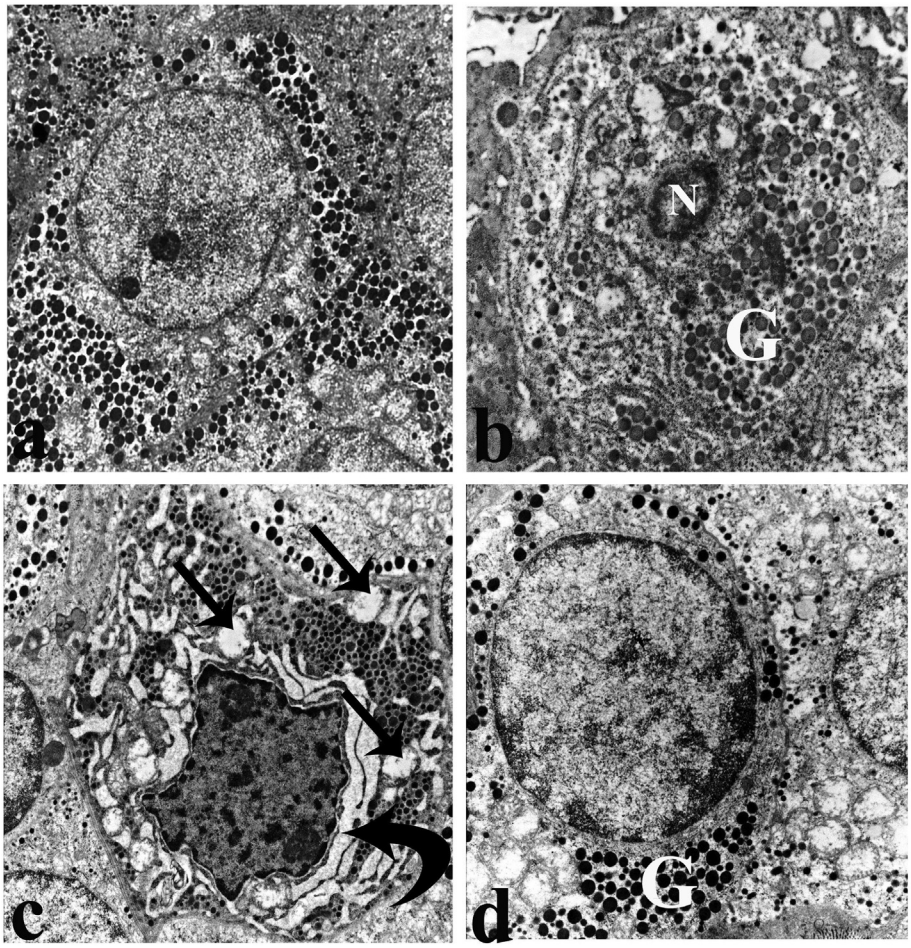

Fig. 9. Electron microscopic picture of gonadotrope of (a) control group showing a healthy gonadotrope (b) mercury-treated group showing a gonadotrope with a shrunken apoptotic nucleus (N) with clogged marginated chromatin. The cell shows degeneration of the cytoplasmic organelles and secretory granules (G). (c) Mercury-treated group showing a gonadotrope with marked cytoplasmic rarefaction, mitochondria with cristolysis (arrows) and dilated endoplasmic reticulum cisterns (curved arrow) (d) mercury-selenium treated group showing a gonadotrope with distinct outline, healthy large nucleus and regenerated secretory granules (G) (x 8000).

expression of the pro-apoptotic markers; Bax, caspase-3 and cytochrome-c at both molecular and tissue levels. This was accompanied by hand in hand increase in the anti-apoptotic Bcl2 expression in the selenium-treated rats relative to the mercury-treated counterparts. This anti-apoptotic action was also evident at histological and ultrastructural level. Those observations support the previous studies elucidating the crucial action of selenium in inhibiting the mitochondrial apoptotic pathway via modulating the apoptotic markers; Bax, Bcl2 and caspases [35–37].

The signaling cascades implicated in the selenium-inhibitory action on apoptosis in the current study seem to be mediated via its antioxidant properties. Several lines of evidence have highlighted the involvement of ROS-mediated apoptosis in methyl-mercury neurotoxicity focusing on the role of ROS in changing the mitochondrial membrane potential, opening the mitochondrial permeability transition pore and releasing apoptogenic factors, such as cytochrome *c* that activate the caspase cascade. The action of selenium in mitigating the mercury-induced oxidative stress-mediated apoptosis was evidenced by significant increase in the activity of the antioxidant enzymes GSH-Px and CAT with subsequent down-regulation of caspase-dependent apoptosis. Another point of complexity in this domain is the fact that mercury induces a “selenium-deficient-like” state, which affects GPx synthesis [38,39] linking caspase activation to ROS generation and redox status.

Modulation of autophagy in the selenium-treated group in the current study was revealed by significant increment in the autophagy related markers; LC3I, LC3II and Beclin 1 denoting significant enhancement of the autophagy process essentially needed for cellular renovation and homeostasis in the adenohypophysis. This was pronounced at ultrastructural level where marked reduction of the myelin figures, multivesicular bodies and autophagic vacuoles was observed. A mechanistic insight into the role of selenium in improving autophagy dysfunction after Hg exposure in the current study appears to be mediated via its action in enhancing the antioxidant defense and redox homeostasis. This was evidenced by activation of the GSH peroxidase and catalase antioxidant system that essentially leads to a more efficient free radical scavenging ability of the adenohypophysis. The modern prospective that autophagy is actually considered a crucial cellular antioxidant pathway [40] supports our hypothesis.

A well-characterized regulatory event in autophagy and apoptosis is the interaction of Beclin-1 with Bcl-2 where Beclin-1 activity is inhibited by interaction with Bcl-2 [18], thus apoptosis enhancement together with autophagy impairment noticed in the current study could well be explained by the regulatory role of Beclin 1.

Selection between cell survival and death in the context of mercury-induced pituitary intoxication in the current study seem to be interceded through caspase-mediated cleavage of Beclin 1 which promotes crosstalk between apoptosis and autophagy through inactivation of Beclin-1-induced autophagy and enhancing apoptosis via promoting the release of proapoptotic factors [18,41,42].

Thus, Bcl-2 plays a dual role in determining cell viability through two principal core machineries: an anti-apoptotic one that inhibits cytochrome *c* release at mitochondrial level, and an autophagy-inhibitory one mediated by interaction with Beclin1 at the endoplasmic reticular level [18,43].

Blockage of autophagy noticed in mercury-treated adenohypophysis could also explain the augmented apoptotic profile in those glands since accumulation of damaged cargo (not eliminated by efficient autophagic machinery) essentially leads to release of pro-apoptotic cell mediators, increasing mitochondrial membrane permeability and promoting cell death.

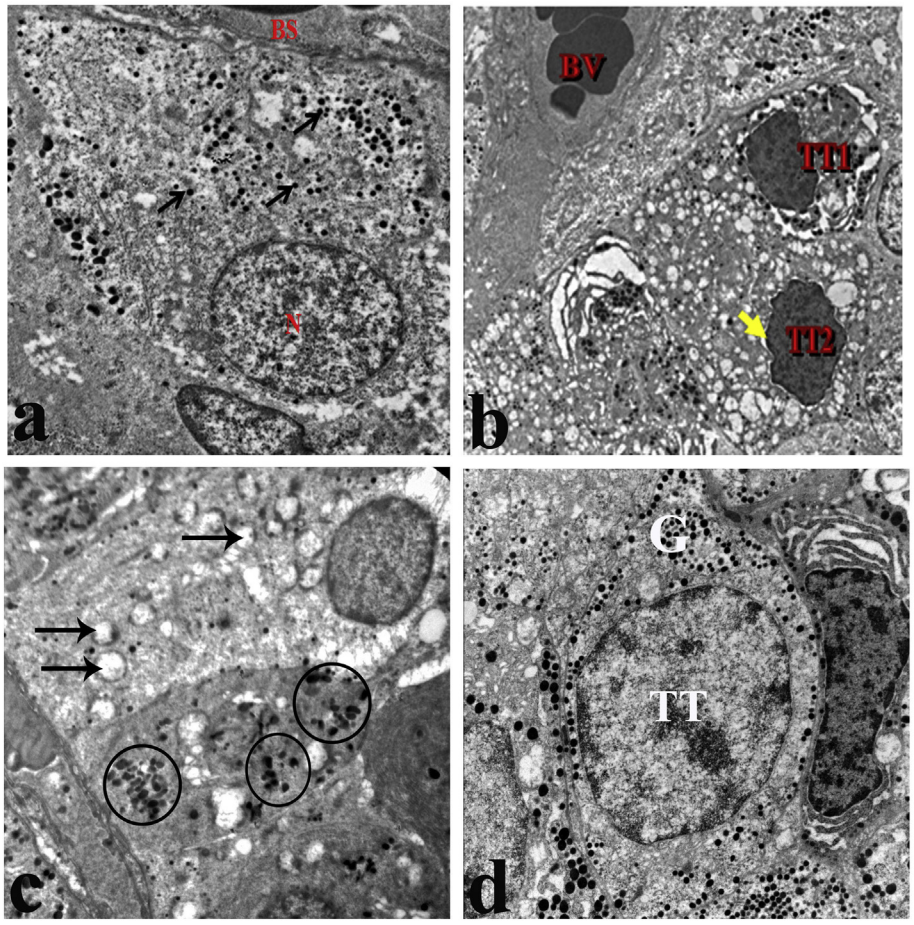

Fig. 10. Electron microscopic picture of thyrotrope of (a) control group showing a thyrotrope in close proximity to a blood sinusoid (BS) with euchromatic rounded nucleus and small-sized secretory granules (arrows)(x 6000) (b) mercury-treated group showing two thyrotropes (TT1, TT2) with a peripherally condensed shrunken nucleus (apoptotic nuclei) and blebby nuclear membrane (yellow arrow). The cytoplasm is heavily studded with cytoplasmic vacuoles (x 5000). (c) Mercury-treated group showing a thyrotrope with many lysosomes (circles) and vacuolated mitochondria (arrows) (x5000) (d) mercury-selenium treated group showing a thyrotroph (TT) with healthy nucleus and preserved secretory granules (G) (x 8000) (BV: blood vessel). (For interpretation of the references to color in this figure legend, the reader is referred to the web version of this article.)

In the present study, the mercury-induced ultrastructural changes were also pronounced in the Folliculostellate cells (Fc) which appeared markedly degenerated with rarified cytoplasm and very few remains cytoplasmic organelles. This structural disintegration essentially necessitates parallel functional disturbances. The Fc also possess a vital scavenger activity by engulfing degenerated cells and play a pivotal role in three broad areas of pituitary function; autocrine/paracrine regulation of anterior pituitary cell function, intra-pituitary communication, and modulation of inflammatory responses [44].

Among the cellular population of the anterior pituitary, the somatotrophs were the most affected cell by mercury toxicity. This could be attributed to the large number and high activity of the somatotroph cell population which make these cells particularly vulnerable to toxicity. The arrangement of these cells along the blood sinusoids and the degree of their vascularization also makes them more vulnerable to extrinsic stimuli.

5. Conclusion

Mercury toxicity caused autophagy dysfunction, induced apoptosis and disrupted the architecture of the adenohypophysis. Those pathological alterations were attributed to disturbing the Beclin1/LC3 and Bax/Bcl2 pathways. Selenium treatment was capable of mitigating most of these deleterious changes and modulating the autophagic and apoptotic milieu of the cells via hampering the ROS-mediated apoptosis. Mechanistic knowledge on the action of selenium on the pituitary disruptive action of mercury paves the way for understanding and targeting therapies for several mercury-induced pituitary diseases and highlights the incrimination of enhanced apoptosis and defective autophagy in this context.

Funding

This research did not receive any specific grant from funding agencies in the public, commercial, or not-for-profit sectors.

Declaration of Competing Interest

The authors declare no conflict of interests.

References

[1] T.W. Clarkson, L. Magos, G.J. Myers, The toxicology of mercury—current exposures and clinical manifestations, N. Engl. J. Med. 349 (18) (2003) 1731–1737.
[2] J.D. Park, W. Zheng, Human exposure and health effects of inorganic and elemental mercury, J. Prev. Med. Public Health 45 (6) (2012) 344.
[3] B. Møller-Madsen, O. Thorlacius-Ussing, (1986). Accumulation of mercury in the anterior pituitary of rats following oral or intraperitoneal administration of methyl mercury, Virchows Arch. B Cell Pathol. 51 (1) (1986) 303.
[4] M. Nylander, Relation between mercury and selenium in pituitary glands of dental staff, Br. J. Ind. Med. 46 (1989) 751–752.
[5] G. Danscher, P. Hørsted-Bindslev, J. Rungby, Traces of mercury in organs from primates with amalgam fillings, Exp. Mol. Pathol. 52 (3) (1990) 291–299.
[6] B. Møller-Madsen, G. Danscher, Localization of mercury in CNS of the rat: IV. The effect of selenium on orally administered organic and inorganic mercury, Toxicol. Appl. Pharmacol. 108 (3) (1991) 457–473.
[7] S.W. Tan, J.C. Meiller, K.R. Mahaffey, The endocrine effects of mercury in humans and wildlife, Crit. Rev. Toxicol. 39 (3) (2009) 228–269.
[8] R.S. Venkatesan, A.M.M. Sadiq, Effect of morin-5′-sulfonic acid sodium salt on the expression of apoptosis related proteins caspase 3, Bax and Bcl 2 due to the mercury induced oxidative stress in albino rats, Biomed. Pharmacother. 85 (2017) 202–208.
[9] F.B. Teixeira, A.C. de Oliveira, L.K. Leão, N.C. Fagundes, R.M. Fernandes, L.M. Fernandes, M.E. Crespo-Lopez, Exposure to inorganic mercury causes oxidative stress, cell death, and functional deficits in the motor cortex, Front. Mol. Neurosci. 11 (2018) 178–192.
[10] F.F. Ferreira, E.M. Nazari, Y.M. Müller, MeHg causes ultrastructural changes in mitochondria and autophagy in the spinal cord cells of chicken embryo, J. Toxicol. (2018) 1–12 2018 Edition.

[11] N. Chen, M. Lin, N. Liu, S. Wang, X. Xiao, Methylmercury-induced testis damage is associated with activation of oxidative stress and germ cell autophagy, J. Inorg. Biochem. 190 (2019) 67–74.
[12] A.G. Porter, R.U. Jänicke, Emerging roles of caspase-3 in apoptosis, Cell Death Differ. 6 (2) (1999) 99.
[13] P.E. Czabotar, G. Lessene, A. Strasser, J.M. Adams, Control of apoptosis by the BCL-2 protein family: implications for physiology and therapy, Nat. Rev. Mol. Cell Biol. 15 (1) (2014) 49.
[14] B. Ku, C. Liang, J.U. Jung, B.H. Oh, Evidence that inhibition of BAX activation by BCL-2 involves its tight and preferential interaction with the BH3 domain of BAX, Cell Res. 21 (4) (2011) 627.
[15] D. Glick, S. Barth, K.F. Macleod, Autophagy: cellular and molecular mechanisms, J. Pathol. 221 (1) (2010) 3–12.
[16] J. Yang, Y. Zhang, S. Hamid, J. Cai, Q. Liu, H. Li, R. Zhao, H. Wang, S. Xu, Z. Zhang, Interplay between autophagy and apoptosis in selenium deficient cardiomyocytes in chicken, J. Inorg. Biochem. 170 (2017) 17–25.
[17] S. Erlich, L. Mizrachy, O. Segev, L. Lindenboim, O. Zmira, S. Adi-Harel, J.A. Hirsch, R. Stein, R. Pinkas-Kramarski, Differential interactions between Beclin 1 and Bcl-2 family members, Autophagy 3 (6) (2007) 561–568.
[18] S. Pattingre, A. Tassa, X. Qu, R. Garuti, X.H. Liang, N. Mizushima, M. Packer, M.D. Schneider, B. Levine, Bcl-2 antiapoptotic proteins inhibit Beclin 1-dependent autophagy, Cell 122 (6) (2005) 927–939.
[19] M.V. Rao, A. Purohit, T. Patel, Melatonin protection on mercury-exerted brain toxicity in the rat, Drug Chem. Toxicol. 33 (2) (2010) 209–216.
[20] F.M. Lin, M. Malaiyandi, C. Romero-Sierra, Toxicity of methylmercury: effects on different ages of rats, Bull. Environ. Contam. Toxicol. 14 (2) (1975) 140–148.
[21] J.V. Van, K.B. Meyer, H.J. Olander, G.R. Ruth, Efficacy and safety of selenium-vitamin E injections in newborn pigs to prevent subclinical deficiency in growing swine, Am. J. Vet. Res. 36 (4 Pt. 1) (1975) 387–393.
[22] M. Nazıroğlu, A. Karaoğlu, A.O. Aksoy, Selenium and high dose vitamin E administration protects cisplatin-induced oxidative damage to renal, liver and lens tissues in rats, Toxicology 195 (2–3) (2004) 221–230.
[23] Ergun Karavelioglu, Mehmet Gazi Boyaci, Nejdet Simsek, Mehmet Akif Sonmez, Rabia Koc, Mustafa Karademir, Mustafa Guven, Olcay Eser, Selenium protects cerebral cells by cisplatin induced neurotoxicity, Acta Cir. Bras. 30 (6) (2015) 394–400.
[24] J.D. Bancroft, M. Gamble (Eds.), Theory and Practice of Histological Techniques, Elsevier health sciences, Morgantown, West Virginia, 2008, pp. 601–640.
[25] P. Lee, D.J. Lee, C. Chan, S.W. Chen, I. Ch'en, C. Jamora, Dynamic expression of epidermal caspase 8 simulates a wound healing response, Nature 458 (7237) (2009) 519.
[26] R.F. Beers, I.W. Sizer, A spectrophotometric method for measuring the breakdown of hydrogen peroxide by catalase, J. Biol. Chem. 195 (1952) 133–140.
[27] M.C. Maiuri, G. Le Toumelin, A. Criollo, J.C. Rain, F. Gautier, P. Juin, et al., Functional and physical interaction between Bcl-XL and a BH3-like domain in Beclin-1, EMBO J. 26 (10) (2007) 2527–2539.
[28] M.A. Khan, F. Wang, Reversible dissolution of glutathione-mediated HgSe x S1 − x nanoparticles and possible significance in Hg − Se antagonism, Chem. Res. Toxicol. 22 (11) (2009) 1827–1832.
[29] T. Ikemoto, T. Kunito, H. Tanaka, N. Baba, N. Miyazaki, S. Tanabe, Detoxification mechanism of heavy metals in marine mammals and seabirds: interaction of selenium with mercury, silver, copper, zinc, and cadmium in liver, Arch. Environ. Contam. Toxicol. 47 (3) (2004) 402–413.
[30] R.W. Chen, P.D. Whanger, S.C. Fang, Diversion of mercury binding in rat tissues by selenium-possible mechanism of protection, Pharmacol. Res. Commun. 6 (6) (1974) 571–579.
[31] Ralston NVC & Raymond LJ (2013) Selenium Status and Intake Influences Mercury Exposure Risk in Selenium in the Environment and Human Health. In: Banuelos, Lin, Yin (eds) CRC Press, Atlanta, pp 203–205.
[32] N.V.C. Ralston, Selenium health benefit values as seafood safety criteria, EcoHealth 5 (4) (2008) 442–455.
[33] N.V.C. Ralston, L.J. Raymond, Dietary selenium's protective effects against methylmercury toxicity, Toxicology 278 (1) (2010) 112–123.
[34] L. Raymond, L. Seale, N.C. Ralston, Seafood selenium in relation to assessments of methylmercury exposure risks, in: D.L. Hatfield, M.J. Berry, V.N. Gladyshev (Eds.), Selenium, Springer, New York, 2012, pp. 399–408.
[35] J. Chen, Y. Chu, J. Cao, Z. Yang, X. Guo, Z. Wang, T-2 toxin induces apoptosis, and selenium partly blocks, T-2 toxin induced apoptosis in chondrocytes through modulation of the Bax/Bcl-2 ratio, Food Chem. Toxicol. 44 (4) (2006) 567–573.
[36] Y. Wang, Y. Wu, K. Luo, Y. Liu, M. Zhou, Yan, et al., The protective effects of selenium on cadmium-induced oxidative stress and apoptosis via mitochondria pathway in mice kidney, Food Chem. Toxicol. 58 (2013) 61–67.
[37] M. Nazıroğlu, N. Şenol, V. Ghazizadeh, V. Yürüker, Neuroprotection induced by N-acetylcysteine and selenium against traumatic brain injury-induced apoptosis and calcium entry in hippocampus of rat, Cell. Mol. Neurobiol. 34 (6) (2014) 895–903.
[38] J.L. do Nascimento, K.R. Oliveira, M.E. Crespo-Lopez, B.M. Macchi, L.A. Maues, C. Pinheiro Mda, L.C. Silveira, A.M. Herculano, Methylmercury neurotoxicity & antioxidant defenses, Indian J. Med. Res. 128 (2008) 373–382.
[39] A.E.A. Moneim, Mercury-induced neurotoxicity and neuroprotective effects of berberine, Neural Regen. Res. 10 (6) (2015) 881.
[40] S. Giordano, V. Darley-Usmar, J. Zhang, Autophagy as an essential cellular antioxidant pathway in neurodegenerative disease, Redox Biol. 2 (2014) 82–90.
[41] M. Djavaheri-Mergny, M.C. Maiuri, G. Kroemer, Cross talk between apoptosis and autophagy by caspase-mediated cleavage of Beclin 1, Oncogene 29 (12) (2010) 1717.
[42] E. Wirawan, L.V. Walle, K. Kersse, S. Cornelis, S. Claerhout, I. Vanoverberghe, R. Roelandt, R. De Rycke, J. Verspurten, W. Declercq, P. Agostinis, Caspase-mediated cleavage of Beclin-1 inactivates Beclin-1-induced autophagy and enhances apoptosis by promoting the release of proapoptotic factors from mitochondria, Cell Death Dis. 1 (1) (2011) e18.
[43] B. Levine, S.C. Sinha, G. Kroemer, Bcl-2 family members: dual regulators of apoptosis and autophagy, Autophagy 4 (5) (2008) 600–606.
[44] S. Devnath, K. Inoue, An insight to pituitary folliculo-stellate cells, J. Neuroendocrinol. 20 (6) (2008) 687–691.